

Dual-Specificity Phosphatase 26 Protects Against Nonalcoholic Fatty Liver Disease in Mice Through Transforming Growth Factor Beta–Activated Kinase 1 Suppression

Ping Ye,^{1*} Jijun Liu,^{1*} Wuping Xu,^{3*} Denghai Liu,⁴ Xiangchao Ding,² Sheng Le,² Hao Zhang,² Shanshan Chen,² Manhua Chen,¹ and Jiahong Xia²

Nonalcoholic fatty liver disease (NAFLD), which has a wide global distribution, includes different stages ranging from simple steatosis to nonalcoholic steatohepatitis, advanced fibrosis, and liver cirrhosis according to the degree of severity. Chronic low-grade inflammation, insulin resistance, and lipid accumulation are the leading causes of NAFLD. To date, no effective medicine for NAFLD has been approved by governmental agencies. Our study demonstrated that the expression of dual-specificity phosphatase 26 (Dusp26), a member of the Dusp protein family, was decreased in the liver tissue of mice with hepatic steatosis and genetically obese (ob/ob) mice. In our study, hepatic steatosis, inflammatory responses, and insulin resistance were exacerbated in liver-specific Dusp26-knockout (KO) mice but ameliorated in liver-specific Dusp26-transgenic mice induced by a high-fat diet. In addition, the degree of liver fibrosis was aggravated in high-fat high-cholesterol diet–induced Dusp26-KO mice. We further found that the binding of Dusp26 to transforming growth factor beta–activated kinase 1 (TAK1) to block the phosphorylation of TAK1 regulated the TAK1–p38/c-Jun NH2-terminal kinase signaling axis to alleviate hepatic steatosis and metabolic disturbance. **Conclusion:** These findings suggest that Dusp26 is a good TAK1-dependent therapeutic target for NAFLD. (HEPATOLOGY 2019;69:1946–1964).

Nonalcoholic fatty liver disease (NAFLD) caused by liver lipid deposition involves progressive steatosis. The progression of steatosis in NAFLD is usually accompanied by hepatitis, fibrosis, cirrhosis, and even hepatocellular carcinoma. NAFLD includes nonalcoholic fatty liver (NAFL)

Abbreviations: Acaca, acetyl-coenzyme A carboxylase 1; ALT, alanine aminotransferase; AST, aspartate aminotransferase; Ca, constitutively active; Ccl2, chemokine (C-C motif) ligand 2; Cxcl10, chemokine (C-X-C motif) ligand 10; Dusp26, dual-specificity phosphatase 26; ERK, extracellular signal-regulated kinase; FASN, fatty acid synthase; GFP, green fluorescent protein; G6PC, glucose 6-phosphate catalytic subunit; GSK3 β , glycogen synthase kinase 3 beta; GST, glutathione S-transferase; GTT, glucose tolerance test; HA, hemagglutinin; H&E, hematoxylin and eosin; HFD, high-fat diet; HFHC, high-fat, high-cholesterol; HOMA-IR, homeostatic model assessment of insulin resistance; IL, interleukin; IP, immunoprecipitation; IRS1, insulin receptor substrate 1; ITT, insulin tolerance test; JNK, c-Jun NH2-terminal kinase; KO, knockout; lenti, lentiviral; LW/BW, liver weight-to-body weight ratio; MAPK, mitogen-activated protein kinase; MEK, MAP kinase-ERK kinase; MKK, putative mitogen activated protein kinase; NAFLD, nonalcoholic fatty liver disease; NASH, nonalcoholic steatohepatitis; NCD, normal chow diet; NEFA, nonesterified fatty acid; NF- κ B, nuclear factor kappa B; NTG, nontransgenic; PA, palmitic acid; PCK1, phosphoenolpyruvate carboxykinase 1; PPAR α , peroxisome proliferator-activated receptor alpha; TAK1, transforming growth factor beta–activated kinase 1; TBK1, TANK-binding kinase 1; TC, total cholesterol; TG, triglyceride; TNF, tumor necrosis factor; WT, wild type.

Received August 18, 2018; accepted December 12, 2018.

Additional Supporting Information may be found at onlinelibrary.wiley.com/doi/10.1002/hep.30485/supinfo.

*These authors contributed equally to this work.

Supported by grants from the National Natural Science Foundation of China (81730015, 81470482, and 81600186).

© 2018 The Authors. HEPATOLOGY published by Wiley Periodicals, Inc. on behalf of American Association for the Study of Liver Diseases. This is an open access article under the terms of the Creative Commons Attribution-NonCommercial License, which permits use, distribution and reproduction in any medium, provided the original work is properly cited and is not used for commercial purposes.

and nonalcoholic steatohepatitis (NASH). NAFL is characterized by steatosis of the liver without hepatocyte injury, and NASH is characterized by hepatocyte injury against a background of steatosis in the process of necroinflammation.⁽¹⁻³⁾ In the twenty-first century, NAFLD has become a prevalent disease that affects approximately 1 billion individuals worldwide.⁽⁴⁾ It is estimated that NAFLD is to be the main reason for liver failure in the next decade. A series of metabolic risk factors including insulin resistance, dyslipidemia, and obesity may be associated with NAFLD.⁽⁵⁾ However, the specific mechanism and effective therapeutic method remain unclear.^(5,6)

Dual-specificity phosphatases (DUSPs) play a key role in the cellular signaling pathways that regulate the growth, differentiation, and apoptosis of cells by means of dephosphorylating both phosphoserine/threonine and phosphotyrosine on their substrates.^(7,8) Many scientists have demonstrated that several members of the DUSP protein family play potential roles in obesity-associated inflammation or insulin resistance.⁽⁹⁻¹¹⁾ Dusp9, a member of the DUSP protein family, was down-regulated in the mitogen-activated protein kinase (MAPK) pathway to regulate differentiation, proliferation, and apoptosis through a series of cellular responses. Dusp26 was reported to inhibit the phosphorylation of p38 to block p38-mediated apoptosis in some types of tumor cells.⁽¹²⁻¹⁴⁾ We hypothesized

that Dusp26 may play a critical role in the lipid accumulation and obesity-associated inflammation in liver cells during the progression of different stages of NAFLD. In our study, the expression of Dusp26 was dramatically decreased in the liver tissue of high-fat diet (HFD)-induced mice. Conditional liver-specific Dusp26-knockout (KO) mice and Dusp26-transgenic mice were used to clarify how Dusp26 affects NAFLD in mice under the pathological conditions associated with obesity.

Materials and Methods

ANIMAL LIVER SAMPLES

Adult male mice (C57BL/6), 8-10 weeks of age (17-27 g), were housed at $25 \pm 5^\circ\text{C}$ under a 12-hour light/dark cycle with free access to water and food. The mice were fed an HFD (60.9% fat, 21.8% carbohydrate, and 18.3% protein; D12492; Research Diets) for different weeks and a high-fat, high-cholesterol (HFHC) diet (42% fat, 44% carbohydrate, 14% protein, and 0.2% cholesterol; TP26304; Trophic Diets, Nantong, China) for 16 weeks, with a normal chow diet (NCD; 4% fat, 78% carbohydrate, and 18% protein; D12450J; Research Diets) for control. Ob/ob mice were fed the NCD for 8 weeks.⁽¹⁴⁾ The animals

View this article online at wileyonlinelibrary.com.

DOI 10.1002/hep.30485

Potential conflict of interest: Nothing to report.

ARTICLE INFORMATION:

From the ¹Department of Cardiology, The Central Hospital of Wuhan, Tongji Medical College, Huazhong University of Science and Technology, Wuhan, China; ²Department of Cardiovascular Surgery, Union Hospital, Tongji Medical College, Huazhong University of Science and Technology, Wuhan, China; ³Department of Neurology, The Central Hospital of Wuhan, Tongji Medical College, Huazhong University of Science and Technology, Wuhan, China; ⁴Department of Cardiology, The Central Hospital of Wuhan, School of Medicine, Jiangnan University, Wuhan, China.

ADDRESS CORRESPONDENCE AND REPRINT REQUESTS TO:

Jiahong Xia, M.D., Ph.D.
Department of Cardiovascular Surgery, Union Hospital
Tongji Medical College
Huazhong University of Science and Technology
No. 1277, Jiefang Road
Wuhan 430022, China
E-mail: jiahong.xia@hust.edu.cn
or

Manhua Chen, M.D., Ph.D.
Department of Cardiology, Central Hospital of Wuhan
Tongji Medical College, Huazhong University of Science and
Technology
No. 26 Shengli Street
Wuhan 430014, China
E-mail: cmh_centre@163.com

were bred and maintained in a specific pathogen-free barrier facility at Tongji Medical College (Wuhan, China). All animal experiments were approved by the Institutional Animal Care and Use Committee of Tongji Medical College.

WESTERN BLOT

Total protein was isolated from tissues or cells. Protein (40–50 μ g) was subjected to a 10% sodium dodecyl sulfate–polyacrylamide gel electrophoresis gel, transferred to a polyvinylidene difluoride membrane, and incubated with corresponding primary antibodies (Supporting Table S1) overnight at 4°C then incubation with peroxidase-conjugated secondary antibodies (Jackson ImmunoResearch Laboratories; 1:10,000 dilution).

HISTOLOGICAL ANALYSIS AND IMMUNOFLUORESCENCE STAINING

Oil red O staining and hematoxylin and eosin (H&E) staining were performed on frozen and paraffin-embedded liver sections, respectively. Periodic acid–Schiff staining was performed to detect glycogen, as reported.⁽¹⁵⁾ Histological fibrosis was examined by sirius red and alpha-smooth muscle actin staining. To calculate the NAFLD activity score, H&E images ($\times 20$) were analyzed by a trained hepatopathologist who was blinded to the identity of the samples according to criteria described by Kleiner et al.⁽¹⁶⁾ The expression and localization of Dusp26 were investigated by immunofluorescence. Rabbit antimouse–Cd11b antibody (ab75476, 1:100; Abcam) was used to stain infiltrated inflammatory cells in liver sections.

CELL LINES

The human normal hepatocyte cell lines L02 and HEK293T were purchased from the Type Culture Collection of the Chinese Academy of Sciences, Shanghai, China. All cell lines in our laboratory were passaged no more than 30 times after resuscitation and routinely tested for mycoplasma contamination using PCR. Cells were cultured in standard medium comprised of Dulbecco's modified Eagle's medium, 10% fetal bovine serum, and 1% penicillin–streptomycin and placed in 5% CO₂ under a water-saturated atmosphere in a cell incubator at 37°C.

LENTIVIRUS VECTOR CONSTRUCTION

An overexpression plasmid was obtained to construct lentiviral (lenti) DUSP26 virus, and lenti-green fluorescent protein (GFP) was used as control. A constitutively active (Ca) mutant plasmid was obtained to construct lenti-Ca transforming growth factor beta-activated kinase 1 (TAK1) viruses, as described.⁽¹⁷⁾ The lentivirus was packaged using the opti-memori reduced serum medium, pMD2.G, and overexpression plasmids, as well as Polyethyleneimine, and then used to infect 293T cells. Lentivirus supernatant was collected 48 hours later, used to infect L02 cells with polybrene, and then selected by puromycin.

IN VITRO CELL MODEL OF LIPID ACCUMULATION

For the oil-red O staining assay, palmitic acid (PA) and oleic acid stock solution together with 25% bovine serum albumin were mixed and diluted by medium to the indicated concentration. The cells were then stained with 60% oil red O (O1391; Sigma) working solution for 10 minutes to examine the amount of lipid accumulation. Intracellular triglyceride (TG) levels were measured using the commercially available Triglyceride Colorimetric Assay Kit (10010303; Cayman) according to the manufacturer's protocol.

QUANTITATIVE REAL-TIME PCR

Total mRNA was extracted from tissues and cultured and converted to complementary DNA (cDNA). Quantitative real-time PCR amplification was performed with SYBR Green (04887352001; Roche). The mRNA expression levels of related gene expression were normalized against corresponding β -actin expression. The primers used for real-time PCR in this study are presented in Supporting Table S2.

MICE

DUSP26 flox/flox mice were created using the clustered regularly interspaced short palindromic repeats (CRISPR)/CRISPR-associated 9 methods,⁽¹⁵⁾ which were then crossed with albumin–cyclization recombination (Cre) mice (Jackson Laboratory, Bar Harbor, ME) to obtain hepatocyte DUSP26-specific KO mice. Full-length DUSP26 cDNA were inserted after

CAG-loxp-CAT-loxp cassettes, which were microinjected into fertilized embryos (C57BL/6J background) to generate conditional hepatocyte-specific DUSP26 overexpressing mice. Founder mice were crossed with albumin-Cre mice (Jackson Laboratory; 005650) to obtain hepatocyte-specific DUSP26-transgenic mice.

MOUSE EXPERIMENTS

Body weight, fasting blood glucose levels, fasting serum insulin levels, homeostatic model assessment of insulin resistance (HOMA-IR) values, glucose tolerance tests (GTTs), and insulin tolerance tests (ITTs) were examined and performed as described.⁽¹⁵⁾

MOUSE HEPATIC LIPID AND LIVER FUNCTION ASSAY

Liver tissue TG, total cholesterol (TC), and non-esterified fatty acid (NEFA) levels were measured using commercial kits (Wako, Osaka, Japan), while liver functions were evaluated in the animals by determining the serum concentrations of alanine aminotransferase (ALT), aspartate aminotransferase (AST), and alkaline phosphatase using an ADVIA 2400 Chemistry System analyzer (Siemens, Tarrytown, NY), according to the manufacturer's instructions.

PLASMID CONSTRUCTS

Full-length sequences for the human DUSP26 coding region were cloned into pcDNA5-hemagglutinin (HA) and phage-Flag vectors to generate the pcDNA5-HA-DUSP26 and phage-Flag-DUSP26 recombinant plasmids. The DUSP26 coding region was cloned into a vector which contains glutathione *S*-transferase (GST)-HA to get GST-HA-DUSP26. DUSP26 truncations were obtained through PCR amplification using corresponding primer pairs. In the same way, the pcDNA5-HA-TAK1, pcDNA5-Flag-TAK1, and Flag-labeled TAK1 truncations were constructed. Primers used to generate these constructs are listed in Supporting Table S4.

IMMUNOPRECIPITATION AND GST PRECIPITATION ASSAYS

Immunoprecipitation (IP) assays were performed as described to identify the binding capacity and domain

of DUSP26 that binds to TAK1.⁽¹⁸⁾ GST precipitation assays were performed as described.⁽¹⁹⁾

GST PRECIPITATION ASSAYS

Direct interaction between DUSP26 and TAK1 was determined using a GST precipitation assay.⁽⁹⁾ Briefly, Rosetta (DE3) *Escherichia coli* cells were transformed with the vector pGEX-4T-1-GST-DUSP26, and then expression was induced using 0.5 mM isopropyl- β -D-thiogalactopyranoside. The *E. coli* were lysed, and the extracts were incubated with glutathione-Sepharose 4B beads at 4°C for 1 hour. The beads were then incubated with purified Flag-tagged TAK1, which was prepared through IP, for an additional 4 hours. Proteins that had interacted were eluted in elution buffer (50 mM Tris-HCl [pH 8.0] and 20 mM reduced glutathione) and subjected to immunoblotting using anti-Flag antibodies. Extracts from *E. coli* expressing only a GST tag were used as the negative control.

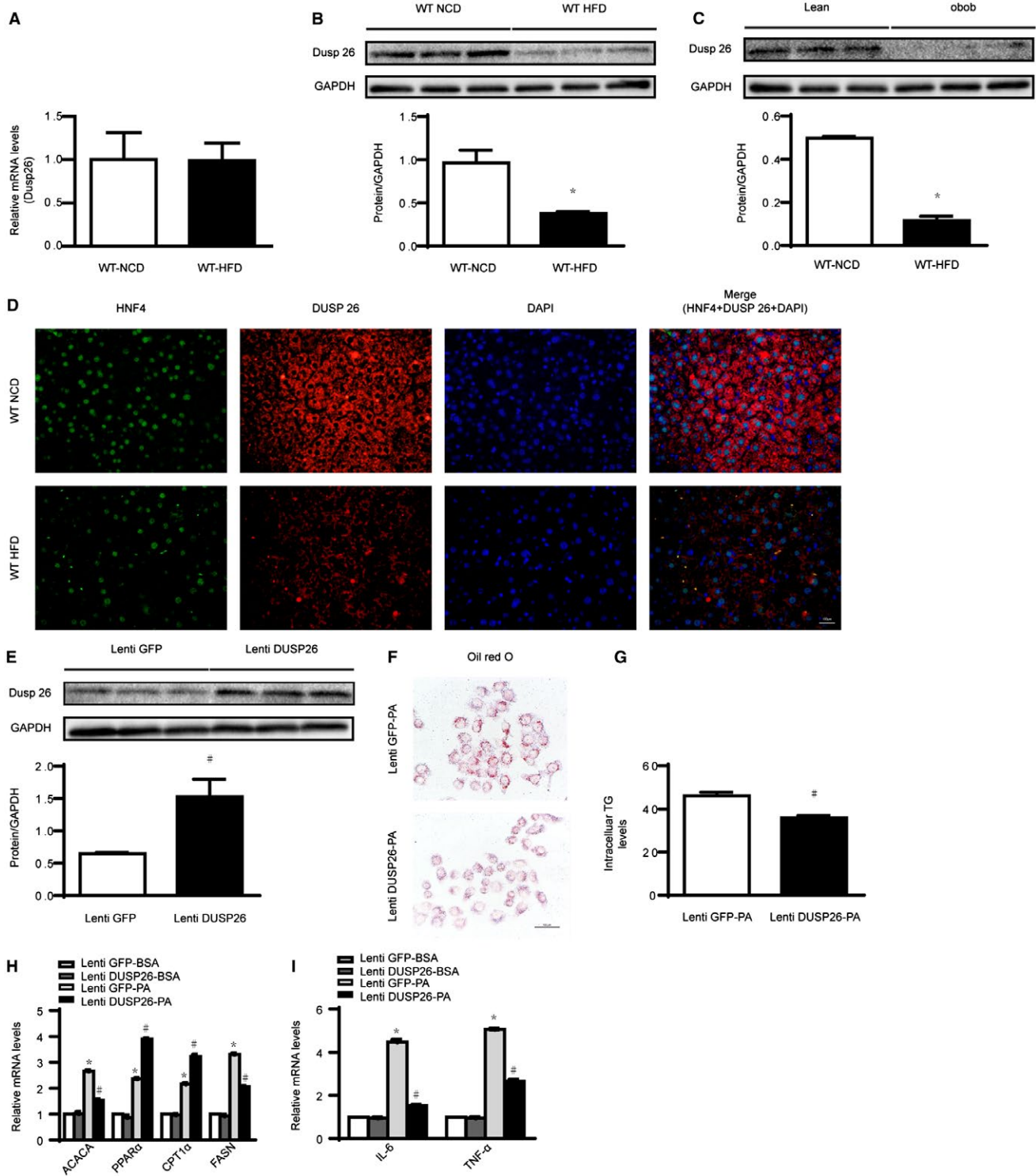
STATISTICAL ANALYSIS

All data are presented as mean \pm SD. Differences between two groups were determined using the two-tailed Student *t* test, and differences among three groups or more were evaluated by one-way analysis of variance, followed by Tukey's *post hoc* test for data meeting homogeneity of variance or with Tamhane's T2 analysis for data of heteroscedasticity. *P* < 0.05 was considered statistically significant.

Results

Dusp26 PROTEIN EXPRESSION IS DOWN-REGULATED IN HFD-INDUCED AND GENETICALLY OBESE MICE

To clarify the relationship between Dusp26 and metabolic disease in the liver, the mRNA expression of Dusp26 was measured, and the result showed that there were no significant differences between NCD-induced and HFD-induced mice (Fig. 1A). However, the protein expression of Dusp26 in liver samples from HFD-induced mice was down-regulated compared with that in NCD-induced mice (Fig. 1B). In



agreement with this, ob/ob mice also had lower expression of Dusp26 than lean mice (Fig. 1C). In addition, immunofluorescence on liver sections further proved

that the expression of Dusp26 is decreased in livers with hepatic steatosis (Fig. 1D). The protein expression of Dusp26 was decreased in HFD-induced and

FIG. 1. Dusp26 protein expression is down-regulated in HFD-induced and genetically obese mice, and overexpression of Dusp26 in human liver cell line L02 attenuated lipid deposition and inflammation induced by palmitate. (A) mRNA expression of Dusp26 in livers of WT mice fed the NCD or HFD for 24 weeks (n = 3). mRNA expression of target genes was normalized to that of β -actin. (B) Protein expression of Dusp26 in livers of WT mice fed the NCD or HFD for 24 weeks (n = 3), * P < 0.05 versus NCD-fed mice. (C) Protein expression of Dusp26 in livers of lean mice and genetically obese mice (ob/ob mice) after 8 weeks of NCD (n = 3), * P < 0.05 versus lean mice. (D) Representative immunofluorescence images of livers of WT mice fed the NCD or HFD for 24 weeks (n = 3), which were stained with antibodies against hepatocyte nuclear factor 4 (green) and Dusp26 (red). 4',6-Diamidino-2-phenylindole (blue) was used to show the nuclei. Scale bar, 100 μ m. (E) Protein expression of Dusp26 in the human liver L02 cell line infected with lenti-GFP or lenti-Dusp26 (n = 3). * P < 0.05 compared with lenti-GFP group. (F,G) Representative oil red O staining (F) and relative intracellular TG levels (G) of L02 cells infected with the indicated lentivirus followed by palmitate stimulation for 24 hours (n = 3 independent experiments, with at least 15 images for each experiment; scale bar, 100 μ m; for the intracellular TG assay, n = 10 for each group). mRNA levels of lipid metabolic (H) and proinflammatory (I) genes in L02 cells infected with the indicated lentivirus followed by palmitate stimulation for 24 hours (n = 3 independent experiments). mRNA expression of target genes was normalized to that of β -actin. * P < 0.05 compared with the bovine serum albumin-treated lenti-GFP group, # P < 0.05 compared with the palmitate-treated lenti-GFP group. Data represent the mean \pm SD. Significance was determined by two-way analysis of variance with general linear model procedures using a univariate approach (H,I) and Student two-tailed, unpaired t test (A-G). Abbreviations: BSA, bovine serum albumin; CPT1 α , carnitine palmitoyltransferase 1 alpha; DAPI, 4',6-diamidino-2-phenylindole; GAPDH, glyceraldehyde 3-phosphate dehydrogenase; HNF4, hepatocyte nuclear factor 4.

ob/ob mice; we speculated that Dusp26 may participate in the pathology of NAFLD.

OVEREXPRESSION OF Dusp26 IN THE HUMAN LIVER CELL LINE L02 ATTENUATED LIPID DEPOSITION AND INFLAMMATION INDUCED BY PALMITATE

To further explore the role of Dusp26 in the progression of NAFLD, we infected L02 cells separately with GFP and Dusp26 by lentivirus to evaluate the effect of Dusp26 on lipid accumulation and the inflammatory response *in vitro*. Western blots showed that Dusp26 was successfully overexpressed in L02 cells (Fig. 1E). Oil red O staining and the levels of intracellular TG indicated that lipid deposition was lower in Dusp26-infected L02 cells than in GFP-infected L02 cells (Fig. 1F,G). The mRNA levels of genes responsible for fatty acid oxidation, such as peroxisome proliferator-activated receptor alpha (PPAR α) and carnitine palmitoyltransferase 1, were much higher in L02 cells infected with Dusp26 than in cells infected with GFP after palmitate treatment; however, expression of the genes related to fatty acid synthesis and inflammation response was lower in L02 cells infected with Dusp26 than in cells infected with GFP after palmitate treatment (Fig. 1H,I).

HEPATOCTE-SPECIFIC Dusp26 DEFICIENCY EXACERBATES HFD-INDUCED OBESITY AND HEPATIC STEATOSIS

To investigate the effect of Dusp26 on hepatic steatosis and its complications, hepatocyte-specific Dusp26-KO mice were generated (Fig. 2A; Supporting Fig. S1A,B). After treatment with the HFD for 24 weeks, the body weight gradually increased in Dusp26-KO and control mice (DUSP26-Flox) compared with the corresponding NCD-induced mice. The weight of Dusp26-KO mice was significantly greater than that of control mice induced by HFD (Fig. 2B). In addition, the liver weight and the liver-to-body weight ratio (LW/BW) were obviously higher in Dusp26-KO mice than in control mice induced by HFD in week 24 (Fig. 2C,D). We found that the lipid contents, including liver tissue TG, TC, and NEFA, were significantly higher in livers of Dusp26-KO mice than in control mice after the administration of HFD for 24 weeks (Fig. 2E-G). Moreover, the mRNA expression levels of fatty acid synthase (FASN), acetyl-coenzyme A (CoA) carboxylase 1 (Acaca), fatty acid uptake (cluster of differentiation 36 [CD36]), fatty acid transport protein 1 (FATP1), and cholesterol synthesis sterol regulatory element-binding protein-1c (SREBP-1) were significantly up-regulated in the livers of Dusp26-KO mice, whereas the expression levels of medium-chain acyl-CoA dehydrogenase (Mcad) and PPAR α were much lower in the Dusp26-KO mice than in the

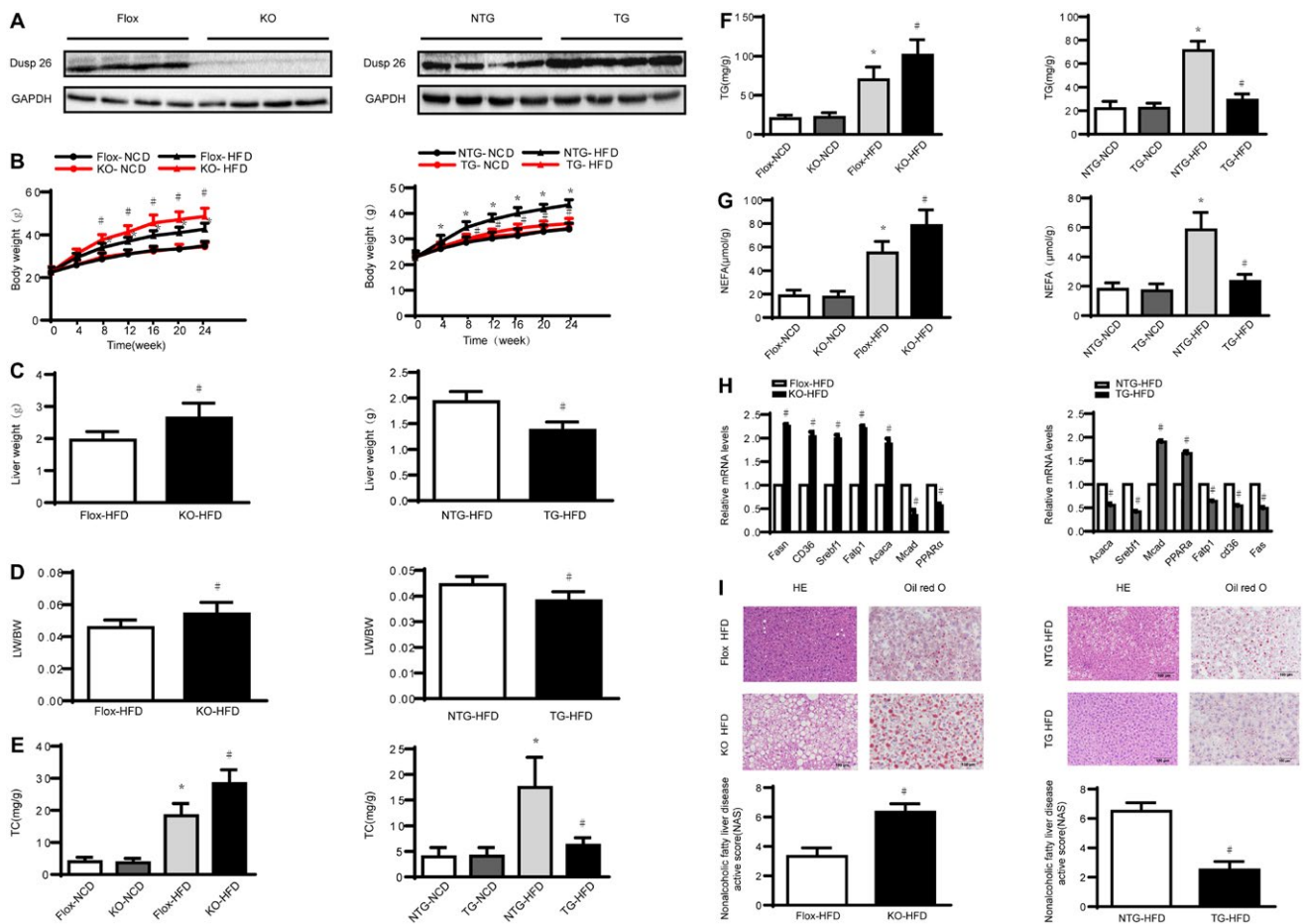


FIG. 2. HFD-induced obesity and hepatic steatosis exacerbated by hepatocyte-specific Dusp26 deficiency and reversed by hepatocyte-specific Dusp26 overexpression. (A) Protein expression of Dusp26 in the livers of Dusp26-KO (left), Dusp26-transgenic (right), and control mice (n = 3). (B) Body weight change in Dusp26-KO (left), Dusp26-transgenic (right), and control mice administered the HFD or NCD for 24 weeks (n = 8). (C,D) Liver weight (C) and LW/BW ratio of Dusp26-KO, Dusp26-transgenic, and control mice (D) at 24 weeks after HFD administration (n = 8). (E-G) Hepatic TC, TG, and NEFA contents of mice in livers of indicated groups were measured by commercial kits (n = 8). (H) mRNA expression of genes associated with fatty acid uptake and synthesis and oxidation in the liver samples of Dusp26-KO (left), Dusp26-transgenic (right), and control mice after 24 weeks of HFD treatment (n = 4). (I) H&E (upper) and oil red O (bottom) staining of liver sections of Dusp26-KO (left), Dusp26-transgenic (right), and control mice after HFD treatment (n = 6). Scale bar, 100 μm. Data represent the mean ± SD. **P* < 0.05 versus Flox/NCD group, NTG/NCD group; #*P* < 0.05 versus Flox/HFD group, NTG/HFD group. Significance was determined by two-way analysis of variance with general linear model procedures using a univariate approach (B,E-G) and Student two-tailed, unpaired *t* test (C,D,H,I). Abbreviations: GAPDH, glyceraldehyde 3-phosphate dehydrogenase; NAS, NAFLD activity score.

control mice after 24 weeks of HFD administration (Fig. 2H). Furthermore, the results of H&E and oil red O staining of liver sections also indicated that lipid deposition in the liver tissue significantly increased in the Dusp26-KO group compared with that in the control group after 24 weeks of HFD administration (Fig. 2I).

Dusp26 OVEREXPRESSION INHIBITS HFD-INDUCED OBESITY AND HEPATIC STEATOSIS

We constructed hepatocyte-specific Dusp26-transgenic mice to investigate the function of Dusp26 overexpression on HFD-induced obesity and hepatic

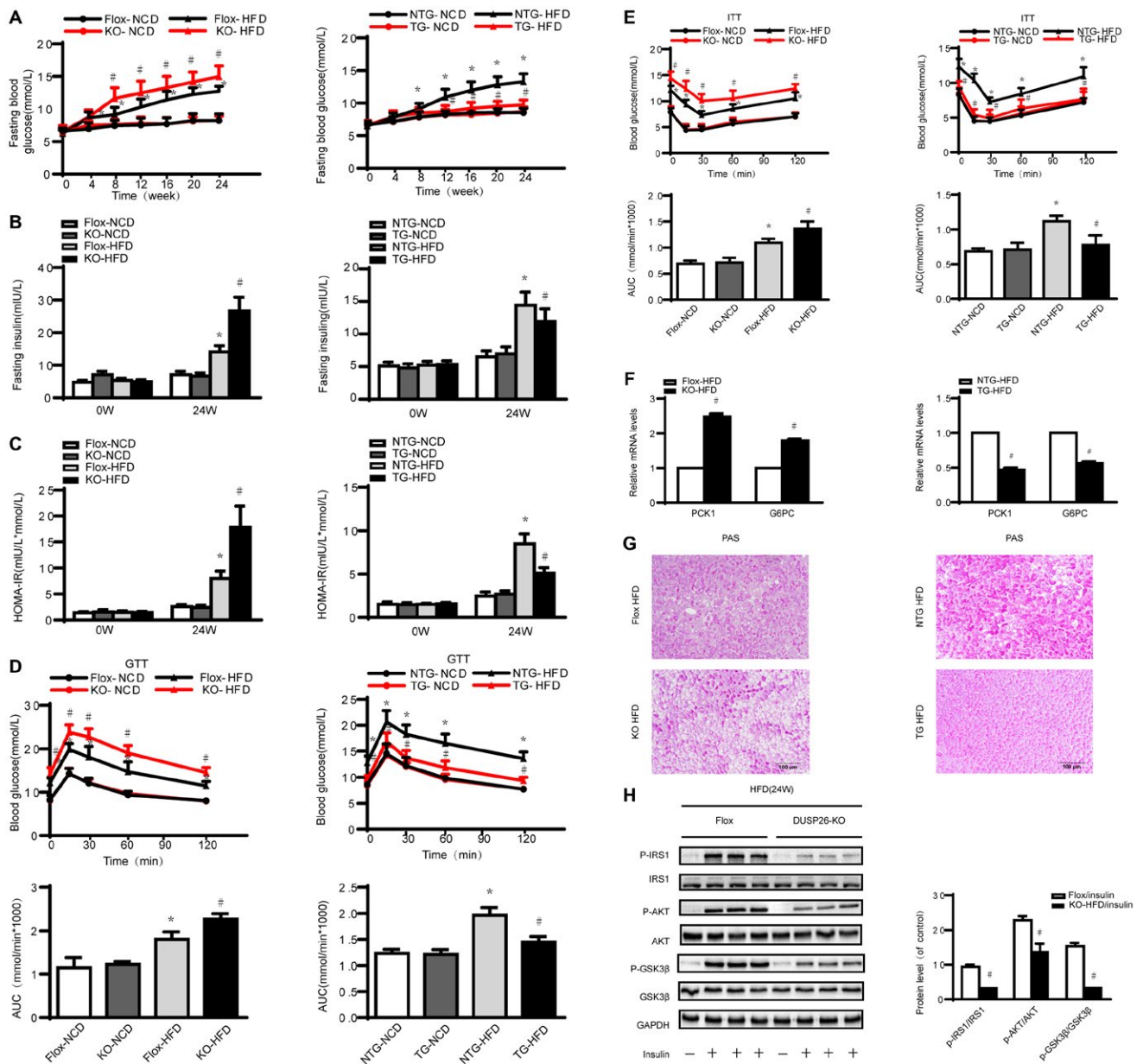


FIG. 3. Insulin resistance was exacerbated by hepatocyte-specific *Dusp26* deficiency and inhibited by hepatocyte-specific *Dusp26* overexpression induced by HFD. (A–C) Fasting blood glucose (A), fasting insulin (B), and HOMA-IR (C) in *Dusp26*-KO (left), *Dusp26*-transgenic (right), or control mice treated with the HFD or NCD for 24 weeks. HOMA-IR was calculated as $\text{HOMA-IR} = (\text{fasting blood glucose levels [mmol/L]} \times \text{fasting serum insulin [mIU/L]}) / 22.5$ ($n = 8$). (D,E) Intraperitoneal GTT (1 g/kg) (D) and intraperitoneal ITT (0.75 units/kg) (E) were performed on *Dusp26*-KO (left), *Dusp26*-transgenic (right), and control mice at week 22 or 23 of food administration, respectively. The corresponding area under the curve was calculated ($n = 8$). (F) mRNA levels of PCK1 and G6PC in the livers of mice in the indicated groups ($n = 4$). (G) Representative images of periodic acid–Schiff staining on the liver sections of *Dusp26*-KO (left), *Dusp26*-transgenic (right), and control mice after a 24-week HFD treatment ($n = 6$). Scale bar, 100 μm . (H) Representative western blot showing levels of total and phosphorylated IRS1, AKT, and GSK3 β in the livers of *Dusp26*-KO and control mice fed the HFD for 24 weeks; some mice received intraperitoneal insulin injection 10 minutes before liver tissue collection ($n = 3$). Glyceraldehyde 3-phosphate dehydrogenase served as the internal control. Data represent the mean \pm SD. * $P < 0.05$ versus Flox/NCD group or NTG/NCD group; # $P < 0.05$ versus Flox/HFD group or NTG/HFD group. Significance was determined by two-way analysis of variance with general linear model procedures using a univariate approach (A–E) and the Student two-tailed, unpaired t test (F,H). Abbreviations: AUC, area under the curve; GAPDH, glyceraldehyde 3-phosphate dehydrogenase.

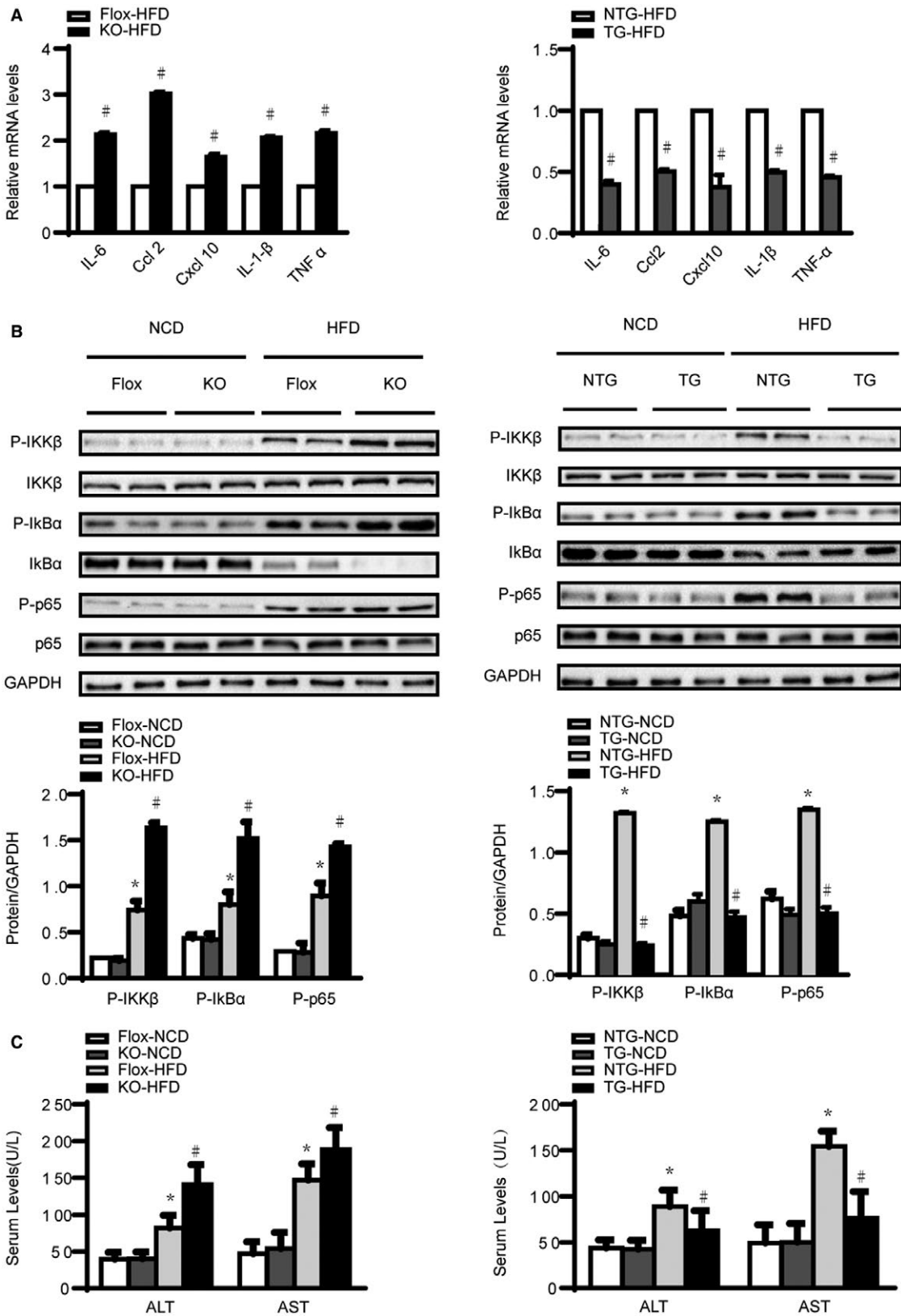


FIG. 4. Inflammatory responses were exacerbated by hepatocyte-specific Dusp26 deficiency and inhibited by hepatocyte-specific Dusp26 overexpression induced by the HFD. (A) mRNA expression levels of inflammatory cytokines and chemokines in the livers of the Dusp26-KO (left) and Dusp26-transgenic (right) groups (n = 4). (B) Expression of key proteins in NF- κ B signaling in the livers of Dusp26-KO (left), Dusp26-transgenic (right), and their corresponding littermate controls after HFD or NCD treatment for 24 weeks. Protein expression was normalized to that of glyceraldehyde 3-phosphate dehydrogenase (n = 4). (C) Serum concentrations of ALT and AST in Dusp26-KO (left), Dusp26-transgenic (right), and their corresponding littermate controls after HFD or NCD treatment for 24 weeks (n = 8). * P < 0.05 versus the Flox/NCD group, NTG/NCD group; # P < 0.05 versus the Flox/HFD group, NTG/HFD group. Data represent the mean \pm SD. Significance was determined by two-way analysis of variance with general linear model procedures using a univariate approach (A) and the Student two-tailed t test (B,C). Abbreviations: GAPDH, glyceraldehyde 3-phosphate dehydrogenase; I κ B, inhibitor of kappa light polypeptide gene enhancer in B cells; IKK, inhibitor of NF- κ B.

steatosis (Fig. 2A; Supporting Fig. S1C). The weight of both groups of mice gradually increased during 24 weeks of HFD administration, the weight of the non-transgenic (NTG) group was obviously greater than that of the Dusp26-transgenic mice. However, no significant difference was found between the two groups of mice fed NCD (Fig. 2B). Then, we harvested the liver and determined the liver weight and LW/BW ratio. The Dusp26-transgenic group had a lower liver weight and LW/BW ratio than the NTG group treated with the HFD (Fig. 2C,D). The lipid contents of TG, TC, and NEFA in the two groups of mice fed the NCD were not significantly different. However, the levels of the TG, TC, and NEFA in the livers of the NTG group were higher than in the Dusp26-transgenic group (Fig. 2E-G). In contrast to the increase in lipid content in Dusp26-KO mice, the liver-specific overexpression of Dusp26 caused an opposite effect on hepatic lipid accumulation. As a consequence, in livers overexpressing Dusp26, the mRNA levels of *FASN*, *Acaca*, *CD36*, *FATP1*, and *SREBP-1* were significantly down-regulated, whereas the expression of *Mcad* and *PPAR α* was higher (Fig. 2H). Moreover, H&E and oil red O staining showed lower hepatic lipid accumulation in the liver tissue of the Dusp26-transgenic group than the NTG group (Fig. 2I).

Dusp26 DEFICIENCY EXACERBATES HFD-INDUCED INSULIN RESISTANCE

To identify the effect of Dusp26 on glucose metabolism, we detected fasting glucose levels and plasma insulin levels and calculated the HOMA-IR indexes.⁽²⁰⁾ HFD-induced Dusp26-KO mice had higher fasting glucose levels, plasma insulin levels, and HOMA-IR indexes than control mice (Fig. 3A-C). Consistently,

Dusp26-KO mice exhibited significantly higher glucose concentrations and areas under the curve in GTT and ITT assays, indicating that DUSP26 deficiency reduced glucose tolerance and insulin sensitivity (Fig. 3D,E). Additionally, the mRNA expression of phosphoenolpyruvate carboxykinase 1 (*PCK1*) and glucose 6-phosphate catalytic subunit (*G6PC*) indicated that gluconeogenesis was higher in the Dusp26-KO group than in the control (Fig. 3F). Consistently, the glycogen content in the Dusp26-KO group was much lower than in control mice after HFD treatment (Fig. 3G), and the phosphorylation levels of key insulin signaling molecules, such as insulin receptor substrate 1 (*IRS1*), *AKT*, and glycogen synthase kinase 3 beta (*GSK3 β*), were considerably attenuated in the liver tissue of Dusp26-KO mice compared with control mice (Fig. 3H).

Dusp26 OVEREXPRESSION INHIBITS HFD-INDUCED INSULIN RESISTANCE

Similarly, we used Dusp26-transgenic mice to prove the function of Dusp26 on glucose metabolism and insulin resistance. Fasting blood glucose was significantly lower in the Dusp26-transgenic mice than in NTG mice after HFD treatment (Fig. 3A). The insulin levels and HOMA-IR index were significantly lower in the Dusp26-transgenic mice (Fig. 3B,C). Correspondingly, the GTT and ITT also showed that the Dusp26-transgenic mice had enhanced glucose tolerance and improve insulin sensitivity (Fig. 3D,E). The expression of *PCK1* and *G6PC* was markedly lower in Dusp26-transgenic mice than in NTG mice (Fig. 3F). Liver sections stained by periodic acid-Schiff after HFD administration also indicated that the amount of glycogen was significantly higher in Dusp26-transgenic mice than in NTG mice (Fig. 3G).

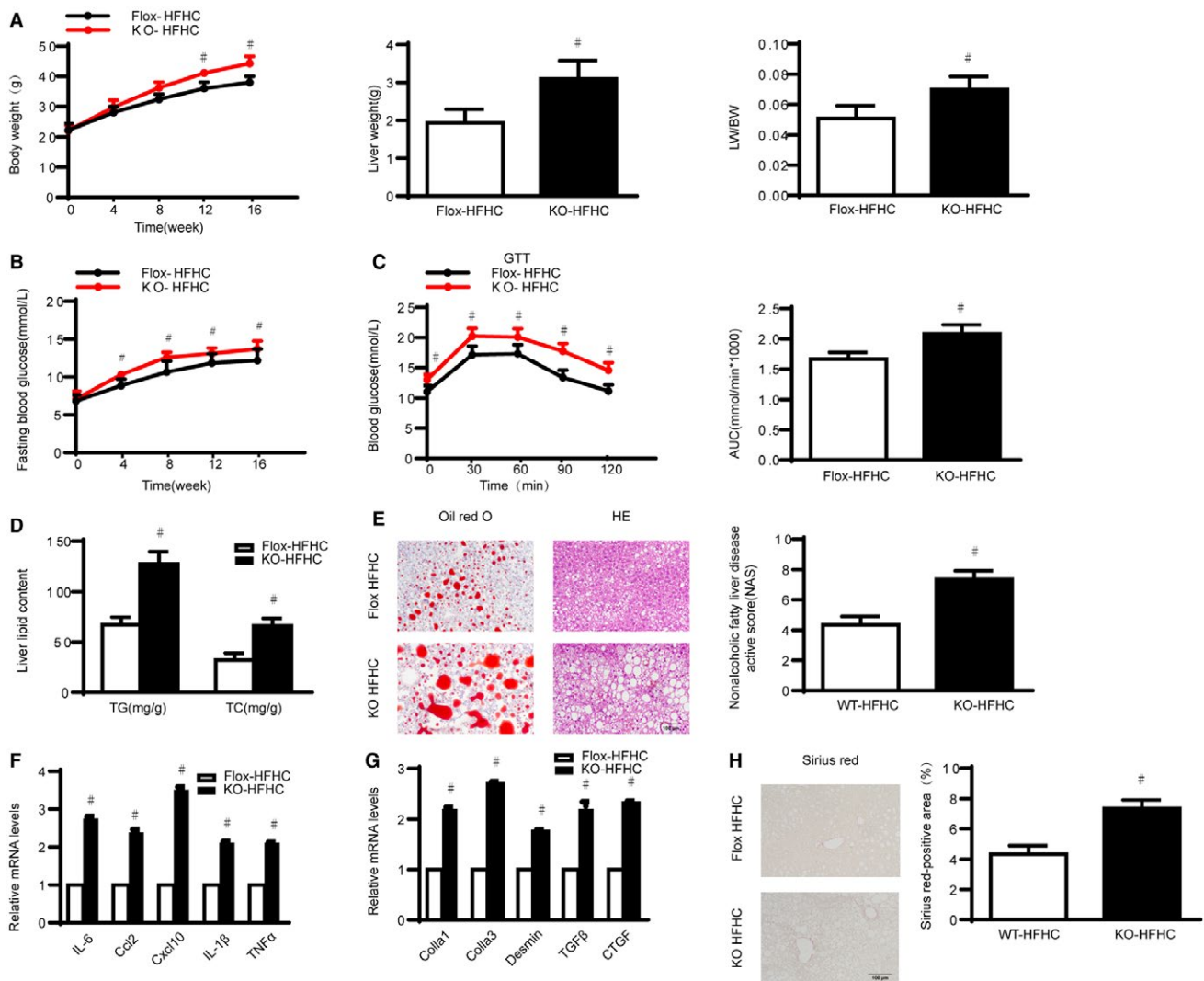


FIG. 5. Hepatocyte *Dusp26* deficiency aggravates lipid accumulation, inflammation and fibrosis, and insulin resistance after HFHC. (A) Changes in body weight, liver weight, and LW/BW of *Dusp26*-KO and control mice treated with the HFHC for 16 weeks ($n = 8$). (B) Fasting blood glucose in *Dusp26*-KO or control mice treated with the HFHC for 16 weeks. Fasting blood glucose levels were measured every 4 weeks. (C) Intraperitoneal GTT (1 g/kg) was performed on *Dusp26*-KO and control mice at week 15 of food administration. (D) Hepatic TG and TC contents of mice in the indicated groups were measured by commercial kits ($n = 8$). (E) Representative images of H&E staining (left) and oil red O staining (right), and liver sections from the indicated mice fed the HFHC diet for 16 weeks ($n = 6$). Scale bar, 100 μ m. (F,G) mRNA levels of proinflammatory (F) and profibrotic genes (G) in the livers ($n = 4$). mRNA expression of the target genes was normalized to that of β -actin. (H) Representative images of picosirius red staining in liver sections from the indicated mice fed the HFHC diet for 16 weeks ($n = 6$). Scale bar, 100 μ m. $^{\#}P < 0.05$ versus the Flox/HFHC group. Data represent the mean \pm SD. Significance was determined by the Student two-tailed t test. Abbreviations: AUC, area under the curve; *Coll1a1*, collagen type I alpha 1 chain; *CTGF*, connective tissue growth factor; NAS, NAFLD activity score.

Dusp26 DEFICIENCY EXACERBATES HFD-INDUCED INFLAMMATORY RESPONSE

Given that chronic inflammation is also associated with NAFLD, we examined the expression

of proinflammatory factors such as interleukin 6 (IL-6), chemokine (C-C motif) ligand 2 (*Ccl2*), chemokine (C-X-C motif) ligand (*Cxcl10*), IL-1 β , and tumor necrosis factor alpha (TNF α). Compared with the control group, the expression of inflammatory response markers was up-regulated in *Dusp26*-KO

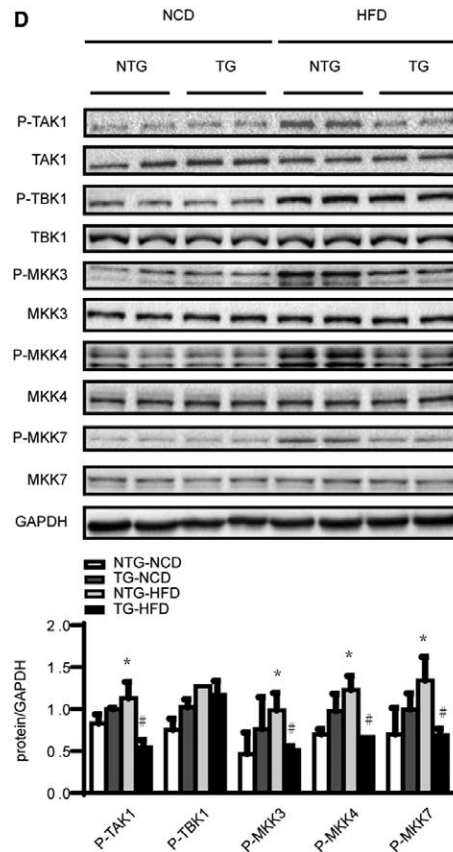
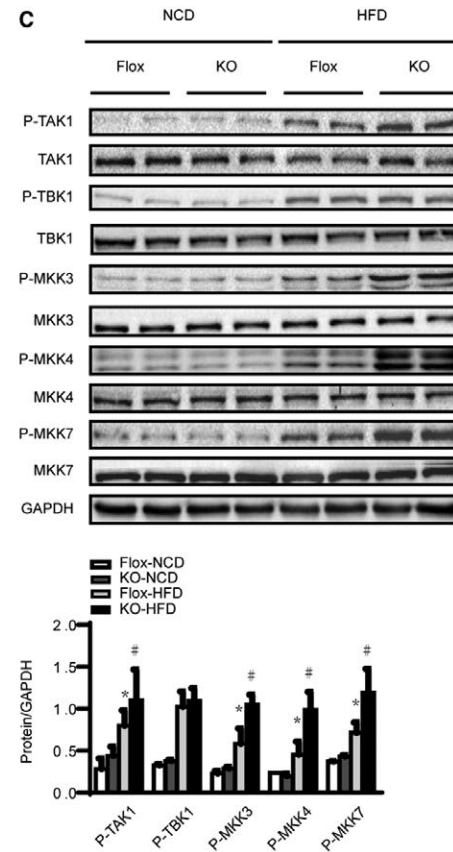
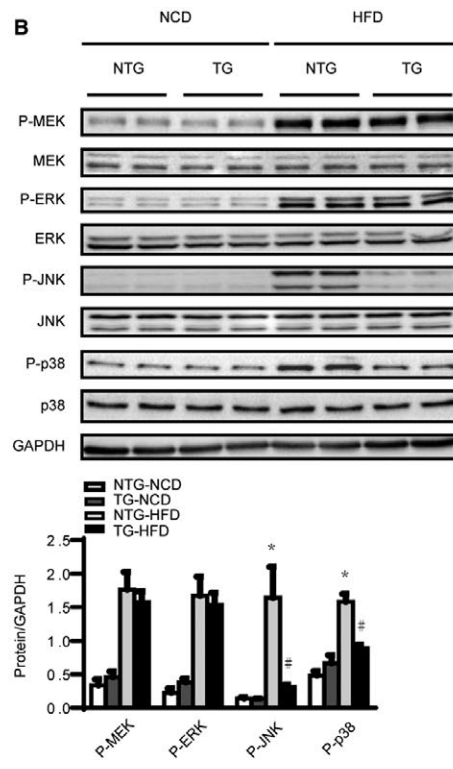
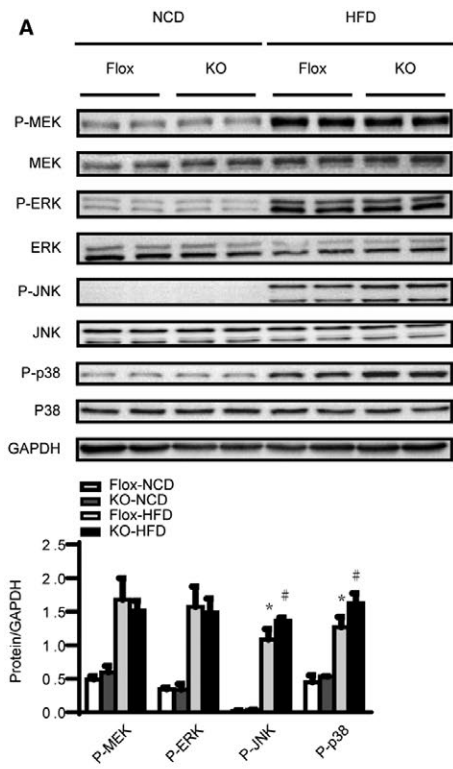


FIG. 6. TAK1 and its downstream pathways are involved in Dusp26-regulated hepatic steatosis. (A) MAPK signaling activation was measured by the total and phosphorylated MEK, ERK, JNK, and P38 levels in the livers of Dusp26-KO mice and their control littermates after HFD treatment for 24 weeks ($n = 3$). Protein expression was normalized to that of GAPDH. (B) MAPK signaling activation was measured by the total and phosphorylated MEK, ERK, JNK and P38 levels in the livers of Dusp26-transgenic mice and their control littermates after HFD treatment for 24 weeks ($n = 3$). Protein expression was normalized to that of GAPDH. (C) JNK and P38 upstream signaling activation was measured from the total and phosphorylated TAK1, TBK1, MKK3, MKK4 and MKK7 levels in the livers of Dusp26-KO mice and their control littermates after HFD treatment for 24 weeks ($n = 3$). Protein expression was normalized to that of glyceraldehyde 3-phosphate dehydrogenase. (D) JNK and P38 upstream signaling activation was measured from the total and phosphorylated TAK1, TBK1, MKK3, MKK4, and MKK7 levels in the livers of Dusp26-transgenic mice and their control littermates after HFD treatment for 24 weeks ($n = 3$). Protein expression was normalized to that of glyceraldehyde 3-phosphate dehydrogenase. * $P < 0.05$ versus Flox/NCD group, NTG/NCD group; # $P < 0.05$ versus Flox/HFD group, NTG/NCD group. Data represent the mean \pm SD. Significance was determined by two-way analysis of variance with general linear model procedures using a univariate approach. Abbreviations: GAPDH, glyceraldehyde 3-phosphate dehydrogenase.

mice after 24 weeks of HFD administration (Fig. 4A). Exorbitant activation of nuclear factor kappa B (NF- κ B) signaling in mice was also associated with insulin resistance and the production of inflammatory cytokines in hepatocytes.⁽²¹⁾ Western blotting showed that NF- κ B signaling was significantly activated in Dusp26-KO mice (Fig. 4B). In addition, plasma levels of ALT and AST were detected as markers of liver function and compared with those of the control mice; the levels of liver function markers were elevated in Dusp26-KO mice (Fig. 4C).

Dusp26 OVEREXPRESSION INHIBITS HFD-INDUCED INFLAMMATORY RESPONSE

In the Dusp26-transgenic mice fed the HFD, the mRNA levels of IL-6, Ccl2, Cxcl10, IL-1 β , and TNF α were down-regulated (Fig. 4A). NF- κ B signaling was clearly repressed in Dusp26-transgenic mice (Fig. 4B). In addition, plasma levels of ALT and AST were decreased in Dusp26-transgenic mice (Fig. 4C).

HEPATIC Dusp26 DEFICIENCY EXACERBATES HFHC-INDUCED INFLAMMATION, INSULIN RESISTANCE, AND LIVER FIBROSIS

HFHC food can accelerate the process of NAFLD and promote the transition from simple steatosis to NASH. An HFHC-induced mouse model was constructed to mimic the pathophysiology of NASH in humans. At 12-16 weeks, the body weight was significantly higher in Dusp26-KO mice than in control mice. Unsurprisingly, after a 16-week HFHC

diet, the liver weight and LW/BW ratio were significantly higher in Dusp26-KO mice (Fig. 5A). During weeks 4-16, HFHC-induced Dusp26-KO mice had higher fasting glucose levels than their control counterparts (Fig. 5B). Consistently, GTT results suggested that glucose tolerance was significantly lower in the Dusp26-KO mice than in the control mice (Fig. 5C). We detected that lipid deposition in liver tissue, including TG and TC, was significantly higher in Dusp26-KO mice than in control mice after 16 weeks of HFHC administration (Fig. 5D). And oil red O and H&E staining showed increased lipid accumulation in Dusp26-KO mice (Fig. 5E). In addition, the mRNA expression of inflammatory factors and profibrotic genes was significantly elevated in Dusp26-KO mice compared with the levels in control mice (Fig. 5F,G). The sirius red-stained liver sections showed that the degree of fibrosis were exacerbated in Dusp26-KO mice (Fig. 5H).

TAK1 AND ITS DOWNSTREAM PATHWAYS ARE INVOLVED IN Dusp26-REGULATED STEATOHEPATITIS

MAPK signaling has been reported to be related to several metabolic diseases.⁽²²⁾ We investigated whether MAPK signaling is involved in hepatic steatosis and the relationship between Dusp26 and MAPK signaling. After 24 weeks of HFD administration, compared with the NCD group, the phosphorylation of MAP kinase-ERK kinase (MEK), extracellular signal-regulated kinase 1/2 (ERK1/2), c-Jun NH2-terminal kinase (JNK), and p38 was increased in the HFD group; but only the phosphorylation of JNK and p38 was regulated by the alterations in Dusp26 expression (Fig. 6A,B).

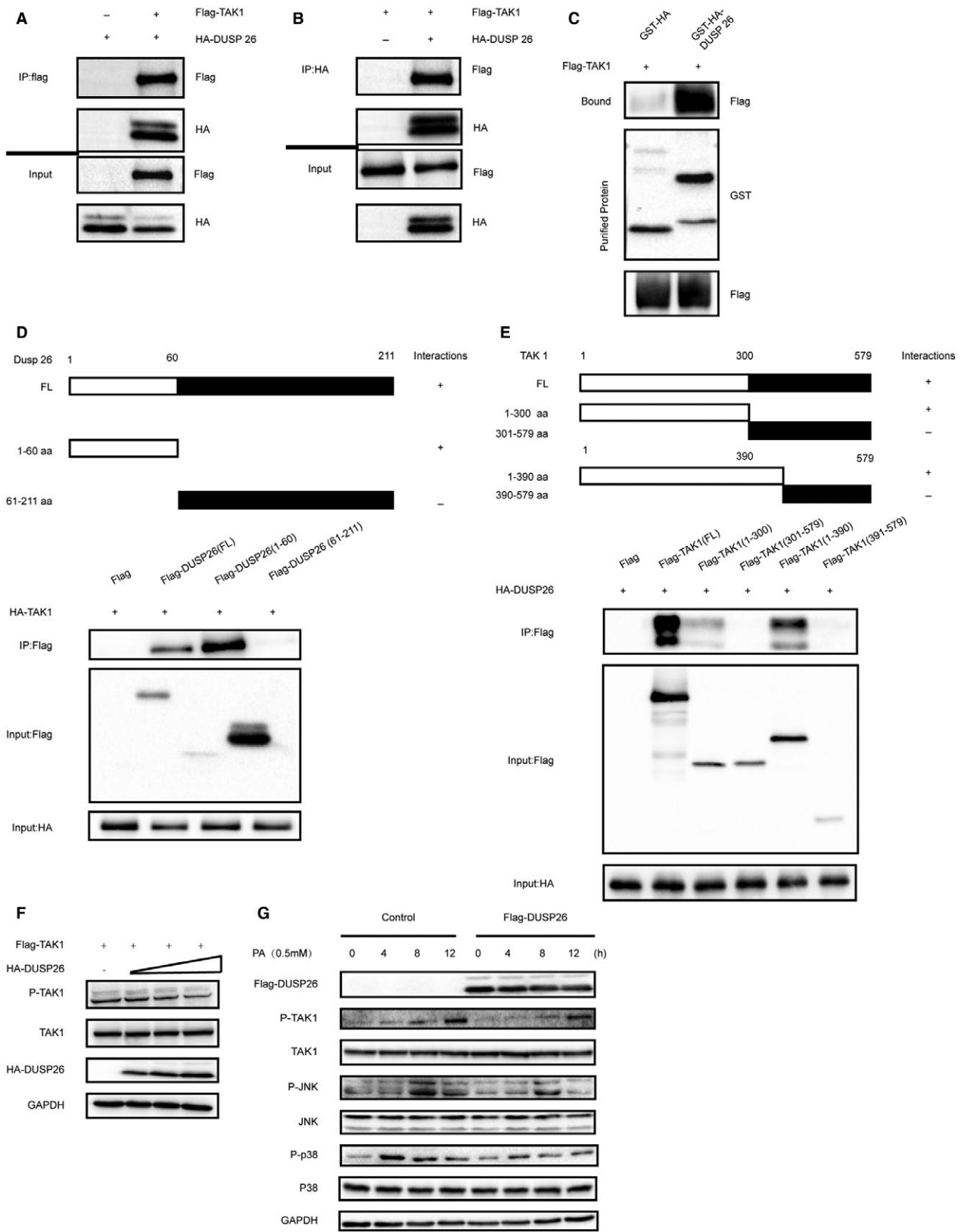


FIG. 7. Dusp26 binds to TAK1 and blocks its phosphorylation. (A,B) A co-IP assay was performed in HEK293T cells cotransfected with Flag-TAK1 and HA-Dusp26 to examine the interaction between TAK1 and Dusp26. (C) GST precipitation assays showing direct Dusp26-TAK1 binding. Purified GST was used as a control. (D,E) The binding domains of Dusp26 and TAK1 were explored using full-length and truncated Dusp26 and TAK1 expression constructs and co-IP assays followed by western blotting. (F) Protein expression of phosphorylation TAK1 was measured in the L02 cell line infected with equal amounts of Flag-TAK1 and a concentration gradient of HA-Dusp26 ($n = 4$). (G) A western blot was performed in the L02 cell line infected with Flag-Dusp26 treated with PA for 0, 4, 8, and 12 hours to examine the protein expression of TAK1 and its downstream pathways. Abbreviations: aa, amino acid; FL, full length; GAPDH, glyceraldehyde 3-phosphate dehydrogenase.

TAK1, TANK-binding kinase 1 (TBK1), and TAK1-related MKK3, MKK4, and MKK7 were potential upstream factors of JNK and p38.^(23,24) We found that only the levels of phosphorylated TAK-1 and TAK-1-related MKK3, MKK4, and MKK7 were changed (Fig. 6C,D).

Dusp26 BINDS TO TAK1 AND BLOCKS ITS PHOSPHORYLATION

A series of IP experiments were performed in the HEK293T cell line to prove that Dusp26 directly interacted with TAK1 to regulate the downstream pathway during the process of NAFLD. Co-IP assays demonstrated that Dusp26 interacts directly with TAK1 (Fig. 7A,B). Additionally, this direct interaction was further validated in a GST pull-down experiment (Fig. 7C). Next, a series of truncated forms of Dusp26 and TAK1 was used for co-IP assays, and the results indicated that the 1-60 amino acid domain of Dusp26 interacted with TAK1 and the 1-300 amino acid domain of TAK1 was responsible for the binding with Dusp26 (Fig. 7D,E).

In order to explore the influence of Dusp26 on TAK1 signaling, the human liver cell line-L02 was infected with equal amounts of Flag-TAK1 and different concentrations of HA-Dusp26. We observed that the expression of TAK1 was inhibited more obviously when the concentration of Dusp26 increased (Fig. 7F). Then we infected L02 cells with Dusp26, and the results demonstrated that expression of the phosphorylation of TAK1, JNK, and p38 was attenuated compared with the control group (Fig. 7G).

TAK1 MEDIATES THE EFFECT OF Dusp26 ON HEPATIC STEATOSIS AND INFLAMMATION INDUCED BY PALMITATE

To further demonstrate whether the effect of Dusp26 on lipid accumulation and inflammation

was mediated by TAK1, L02 cells were infected with GFP, Dusp26, Ca TAK1, or both Dusp26 and Ca TAK1. Western blots showed that phosphorylation of TAK1 and the downstream JNK and p38 was attenuated in Dusp26-overexpressing L02 cells; however, these effects were reversed by overexpression with Ca TAK1 (Fig. 8A). Similarly, oil red O staining and the levels of intracellular TG in L02 cells also suggested that the inhibitory effect of Dusp26 on lipid accumulation was reversed by TAK1 activation (Fig. 8B,C). Consistent with these results, enhancing TAK1 activity completely reversed the regulation of Dusp26 on the mRNA expression of genes involved in fatty acid synthesis beta-oxidation and the inflammatory response (Fig. 8D,E). In order to further state that Dusp26 functioned by modulating TAK1, we then isolated primary hepatocytes from Dusp26-hepatocyte KO mice (Fig. 8F). Oil red O staining showed that the accumulation of lipid in Dusp26-hepatocyte KO mice was reversed by the TAK1 inhibitor 5Z-7-ox (Fig. 8G).

Discussion

According to epidemic reports, the incidence of NAFLD is associated with hepatic insulin resistance. Insulin resistance elevates the levels of insulin in the serum, which causes hepatocytes to increase hepatic lipid synthesis through several insulin-sensitive signaling factors and thereby induces a vicious cycle of inflammation.^(25,26) The metabolism of hepatocytes is disturbed, and insulin signal transduction is impaired, resulting in increased TG storage in liver cells. Thus, the fatty acid input exceeds the output in the liver, resulting in hepatic steatosis.^(27,28) Currently, the number of patients with NAFLD will increase owing to the prevalence of obesity, insulin resistance, and metabolic syndrome.⁽²⁹⁾ Effective therapeutic strategies for NAFLD are limited to changes in lifestyle and the control of dietary intake, and medicine-based approaches have not been proved to have any significant effect on

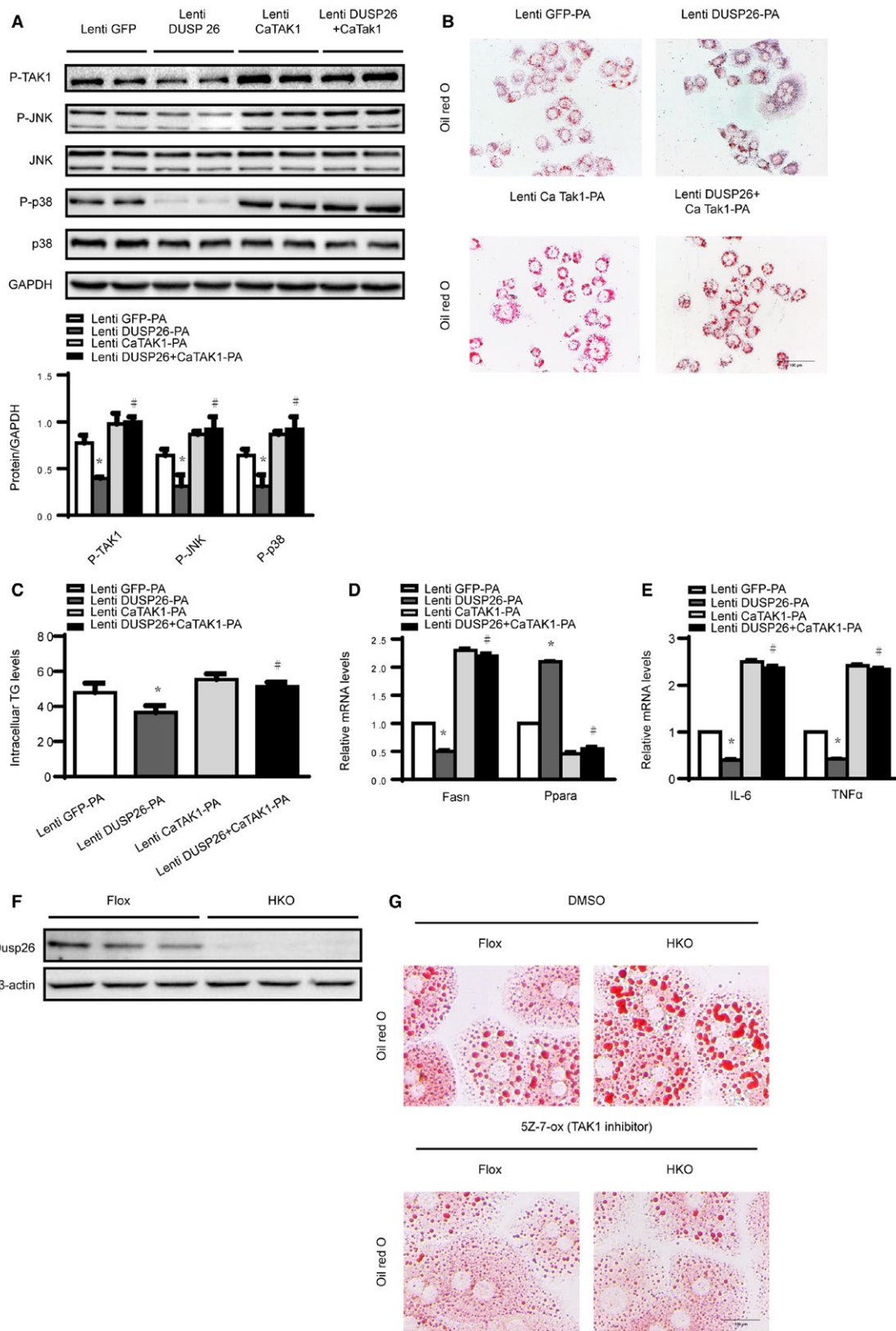


FIG. 8. TAK1 mediates the effect of Dusp26 on hepatic steatosis and inflammation induced by palmitate. (A) Phosphorylated TAK1, JNK, and P38 levels were measured in the L02 cell line treated with palmitate in the indicated groups. Protein expression was normalized to that of glyceraldehyde 3-phosphate dehydrogenase. * $P < 0.05$ compared with the lenti-GFP group, # $P < 0.05$ compared with the lenti-Dusp26 group. (B,C) Representative oil red O staining (B) and relative intracellular TG levels (C) of L02 cells infected with the indicated lentivirus followed by palmitate stimulation for 24 hours ($n = 3$ independent experiments, with at least 15 images for each experiment in B; scale bar, 100 μm ; for the intracellular TG assay in C, $n = 10$ for each group; in bar, one circle represents data from one experiment; scale bar, 100 μm). (D,E) mRNA levels of lipid metabolism (D) and proinflammatory (E) genes in the livers from of mice in the indicated groups ($n = 3$ independent experiments). mRNA expression of target genes was normalized to that of β -actin. * $P < 0.05$ compared with the lenti-GFP group, # $P < 0.05$ compared with the lenti-Dusp26 group. (F) Protein expression of Dusp26 in the livers of Dusp26-KO and control mice ($n = 3$). Protein expression was normalized to that of β -actin. (G) Representative oil red O staining of primary hepatocytes from Dusp26-hepatocyte knockout and control mice followed by PA palmitate stimulation for 24 hours in the absence or presence of shikonin (2.5 μM) ($n = 3$ independent experiments, with at least 15 images for each experiment in G; scale bar, 100 μm). Data represent the mean \pm SD. Significance was determined by the Student two-tailed t test. Abbreviations: DMSO, dimethyl sulfoxide; GAPDH, glyceraldehyde 3-phosphate dehydrogenase; HKO, hepatocyte-specific KO.

NAFLD.⁽³⁰⁾ We demonstrated that Dusp26 played a key role in attenuating HFD-induced lipid accumulation, inflammation, fibrosis, and insulin resistance in hepatocytes in the process of NASH. Our further observations showed that Dusp26 deficiency exacerbated liver fibrosis induced by an HFHC diet. Our present study indicates that Dusp26 may be a therapeutic target for NAFLD and NASH.

Our group observed that the protein expression of Dusp26 was attenuated in the fatty liver tissue compared with normal liver tissue. The DUSP family has been reported to be involved in the innate immune response. It has been reported that the function of Dusp1 is related to several diseases such as inflammatory pathology and diabetes through the ERK1/2–JNK–p38 axis.^(31–33) Cornell et al. demonstrated that Dusp4 deficiency in macrophages reduces the secretion of proinflammatory and anti-inflammatory cytokines through the MAPK signaling pathway.^(34,35) Dusp9 played a key role in the development of NAFLD.⁽¹²⁾ Owing to the different cell types and research contents, the effect of dusp26 on MAPK was variable. Here, we found that DUSP26 modulated NAFLD through the MAPK signaling pathway.

The MAPK signaling pathway played a key role in the development of NAFLD. Lawan and Bennett reported that MAPKs participated in the process of hepatic metabolism, and the perturbation of MAPK/MAPK phosphatase balance would impair insulin action and lipid metabolism in hepatocytes.⁽³⁶⁾ JNK1 phosphorylated the Ser(307) in IRS1 to inhibit the function of the phosphotyrosine-binding domain in regulating insulin signaling.⁽³⁷⁾ Besides, under induction factors such as lipid peroxidation in the steatotic liver, JNK would be activated to increase the transcription

of proinflammatory cytokines through activator protein-1.⁽³⁸⁾ Hepatic gluconeogenesis also depended on the p38 pathway.⁽³⁹⁾ TAK1, a MAPK kinase protein, has been recognized as a common upstream molecule of the MAPK kinase–JNK/p38 and inhibitor of NF- κ B kinase (IKK)–NF- κ B cascades, which plays an indispensable role in hepatic steatosis and related metabolic disorder. It has been reported that during the process of liver injury the activation of TAK1–JNK/NF- κ B impaired the homeostasis of hepatocytes and increased hepatic inflammation, whereas obesity-linked inflammation, hepatic steatosis, and insulin resistance were alleviated in TAK1-deficient mice.^(40,41) The deubiquitinase cylindromatosis, which reversed NASH progression in mice and monkeys, removed the K63-linked polyubiquitin chain of TAK1 to attenuate the activation of the JNK–p38 cascades.⁽⁴²⁾ Ubiquitin-specific protease 18 interacted with TAK1 to suppress the activation of the c-JNK and NF- κ B signaling pathways.⁽¹¹⁾ TNF receptor-associated factor 3, binding to TAK1 to induce the ubiquitination and autophosphorylation of TAK1, regulated the IKK β –NF- κ B and MKK–JNK–IRS1 signaling pathway to alleviate steatosis, insulin resistance, and systemic proinflammatory response in NAFLD.⁽⁴³⁾ Tripartite motif containing 8 also participated in NASH and NAFLD by binding directly to TAK1, which activated the JNK–p38 and NF- κ B pathway.⁽⁴⁴⁾ Here, we showed that Dusp26 alleviated hepatic steatosis and fibrosis, maintained the balance of lipid and glucose metabolism, and decreased the inflammatory response by binding TAK1 and blocking its phosphorylation directly to suppress activation of the MAPK signaling pathway.

However, some reverse effect of TAK1 was reported. Fatty acid oxidation was suppressed and

hepatic steatosis exacerbated in TAK1 liver-specific KO mice.⁽⁴⁴⁾ This conflicting result can be attributed to the difference in the degree of expression of TAK1 in TAK1 knockdown and TAK1 suppression in hepatic steatosis. However, under physiological conditions, TAK1 plays an indispensable role in regulating a wide range of cellular responses. If TAK1 is completely knocked out in the livers of mice, the hepatocytes cannot play the role normally performed by TAK1 in the functional homeostasis of the liver in response to stimuli. Thus, maintaining the expression of TAK1 in a limited range is useful for maintaining functional homeostasis and protecting against steatosis of the liver. Whether the binding of Dusp26 and TAK1 influences other pathways and the reason that the expression of Dusp26 decreases in HFD-induced mice remain elusive.

In conclusion, our current study found that Dusp26 deficiency in hepatocytes activated the downstream p38/JNK pathway by interacting with TAK1. Dusp26 could be a potential target for the treatment of NAFLD. A type of medicine that could enhance the expression of Dusp26 or influence the interaction of Dusp26 and TAK1 would be an effective therapeutic strategy for NAFLD and related metabolic diseases.

REFERENCES

- Benedict M, Zhang X. Non-alcoholic fatty liver disease: an expanded review. *World J Hepatol* 2017;9:715-732.
- Cai J, Zhang X, Li H. Progress and challenges in the prevention and control of nonalcoholic fatty liver disease. *Med Res Rev* 2019;39:328-348.
- Zhang X, She Z, Li H. Time to step-up the fight against NAFLD. *HEPATOLOGY* 2018;67:2068-2071.
- Machado MV. Non-alcoholic fatty liver disease: what the clinician needs to know. *World J Gastroenterol* 2014;20:12956.
- Temple J, Cordero P, Li J, Nguyen V, Oben J. A guide to non-alcoholic fatty liver disease in childhood and adolescence. *Int J Mol Sci* 2016;17:947.
- Clark JM, Diehl AM. Nonalcoholic fatty liver disease: an underrecognized cause of cryptogenic cirrhosis. *JAMA* 2003;289:3000-3004.
- Won E, Lee S, Lee D, Lee D, Bae K, Lee SC, et al. Structural insight into the critical role of the N-terminal region in the catalytic activity of dual-specificity phosphatase 26. *PLoS One* 2016;11:e162115.
- Patterson KI, Brummer T, O'Brien PM, Daly RJ. Dual-specificity phosphatases: critical regulators with diverse cellular targets. *Biochem J* 2009;418:475-489.
- Emanuelli B, Eberle D, Suzuki R, Kahn CR. Overexpression of the dual-specificity phosphatase MKP-4/DUSP-9 protects against stress-induced insulin resistance. *Proc Natl Acad Sci USA* 2008;105:3545-3550.
- Lancaster GI, Kraakman MJ, Kammoun HL, Langley KG, Estevez E, Banerjee A, et al. The dual-specificity phosphatase 2 (DUSP2) does not regulate obesity-associated inflammation or insulin resistance in mice. *PLoS One* 2014;9:e111524.
- Ji Y, Huang Z, Yang X, Wang X, Zhao L, Wang P, et al. The deubiquitinating enzyme cylindromatosis mitigates nonalcoholic steatohepatitis. *Nat Med* 2018;24:213-223.
- Ye P, Xiang M, Liao H, Liu J, Luo H, Wang Y, et al. Dual-specificity phosphatase 9 protects against non-alcoholic fatty liver disease in mice through ASK1 suppression. *HEPATOLOGY* 2018; doi:https://doi.org/10.1002/hep.30198. [Epub ahead of print]
- Pearson G, Robinson F, Beers GT, Xu BE, Karandikar M, Berman K, et al. Mitogen-activated protein (MAP) kinase pathways: regulation and physiological functions. *Endocr Rev* 2001;22:153-183.
- Wang XA, Zhang R, Jiang D, Deng W, Zhang S, Deng S, et al. Interferon regulatory factor 9 protects against hepatic insulin resistance and steatosis in male mice. *HEPATOLOGY* 2013;58:603-616.
- Wang P, Zhang X, Luo P, Jiang X, Zhang P, Guo J, et al. Hepatocyte TRAF3 promotes liver steatosis and systemic insulin resistance through targeting TAK1-dependent signalling. *Nat Commun* 2016;7:10592.
- Kleiner DE, Brunt EM, Van Natta M, Behling C, Contos MJ, Cummings OW, et al. Design and validation of a histological scoring system for nonalcoholic fatty liver disease. *HEPATOLOGY* 2005;41:1313-1321.
- Sakurai H, Nishi A, Sato N, Mizukami J, Miyoshi H, Sugita T. TAK1-TAB1 fusion protein: a novel constitutively active mitogen-activated protein kinase that stimulates AP-1 and NF-KB signaling pathways. *Biochem Biophys Res Commun* 2002;297:1277-1281.
- Zhu LH, Wang A, Luo P, Wang X, Jiang DS, Deng W, et al. Mindin/Spondin 2 inhibits hepatic steatosis, insulin resistance, and obesity via interaction with peroxisome proliferator-activated receptor alpha in mice. *J Hepatol* 2014;60:1046-1054.
- Zhao GN, Zhang P, Gong J, Zhang XJ, Wang PX, Yin M, et al. Tmbim1 is a multivesicular body regulator that protects against non-alcoholic fatty liver disease in mice and monkeys by targeting the lysosomal degradation of Tlr4. *Nat Med* 2017;11:742-752.
- Mousa N, Abdel-Razik A, Sheta T, Shabana W, Zakaria S, Awad M, et al. Serum leptin and homeostasis model assessment-IR as novel predictors of early liver fibrosis in chronic hepatitis B virus infection. *Br J Biomed Sci* 2018;75:192-196.
- Cai D, Yuan M, Frantz DF, Melendez PA, Hansen L, Lee J, et al. Local and systemic insulin resistance resulting from hepatic activation of IKK-beta and NF-kappaB. *Nat Med* 2005;11:183-190.
- Gehart H, Kumpf S, Ittner A, Ricci R. MAPK signalling in cellular metabolism: stress or wellness? *EMBO Rep* 2010;11:834-840.
- Lin D, Li L, Sun Y, Wang W, Wang X, Ye Y, et al. Interleukin-17 regulates the expressions of RANKL and OPG in human periodontal ligament cells via TRAF6/TBK1-JNK/NF-kappaB pathways. *Immunology* 2014;144:472-485.
- Wang C, Chen T, Zhang N, Yang M, Li B, Lü X, et al. Melittin, a major component of bee venom, sensitizes human hepatocellular carcinoma cells to tumor necrosis factor-related apoptosis-inducing ligand (TRAIL)-induced apoptosis by activating CaMKII-TAK1-JNK/p38 and inhibiting IκB kinase-NFκB. *J Biol Chem* 2009;284:3804-3813.
- Farese RJ, Zechner R, Newgard CB, Walther TC. The problem of establishing relationships between hepatic steatosis and hepatic insulin resistance. *Cell Metab* 2012;15:570-573.

- 26) Tilg H, Moschen AR. Insulin resistance, inflammation, and non-alcoholic fatty liver disease. *Trends Endocrinol Metab* 2008;19:371-379.
- 27) Oishi T, Terai S, Kuwashiro S, Fujisawa K, Matsumoto T, Nishina H, et al. Ezetimibe reduces fatty acid quantity in liver and decreased inflammatory cell infiltration and improved NASH in medaka model. *Biochem Biophys Res Commun* 2012;422:22-27.
- 28) Parekh S, Anania FA. Abnormal lipid and glucose metabolism in obesity: implications for nonalcoholic fatty liver disease. *Gastroenterology* 2007;132:2191-2207.
- 29) Torres DM, Harrison SA. Diagnosis and therapy of nonalcoholic steatohepatitis. *Gastroenterology* 2008;134:1682-1698.
- 30) Weiss J, Rau M, Geier A. Non-alcoholic fatty liver disease: epidemiology, clinical course, investigation, and treatment. *Dtsch Arztebl Int* 2014;111:447-452.
- 31) Jeffrey KL, Camps M, Rommel C, Mackay CR. Targeting dual-specificity phosphatases: manipulating MAP kinase signalling and immune responses. *Nat Rev Drug Discov* 2007; 6:391-403.
- 32) Pulido R, Hooft van Huijsduijnen R. Protein tyrosine phosphatases: dual-specificity phosphatases in health and disease. *FEBS J* 2008;275:848-866.
- 33) Wancket LM, Frazier WJ, Liu Y. Mitogen-activated protein kinase phosphatase (MKP)-1 in immunology, physiology, and disease. *Life Sci* 2012;90:237-248.
- 34) Cornell TT, Fleszar A, McHugh W, Blatt NB, Le Vine AM, Shanley TP. Mitogen-activated protein kinase phosphatase 2, MKP-2, regulates early inflammation in acute lung injury. *Am J Physiol Lung Cell Mol Physiol* 2012;303:L251-L258.
- 35) Cornell TT, Rodenhouse P, Cai Q, Sun L, Shanley TP. Mitogen-activated protein kinase phosphatase 2 regulates the inflammatory response in sepsis. *Infect Immun* 2010;78:2868-2876.
- 36) Lawan A, Bennett AM. Mitogen-activated protein kinase regulation in hepatic metabolism. *Trends Endocrinol Metab* 2017;28:868-878.
- 37) Vernia S, Cavanagh-Kyros J, Garcia-Haro L, Sabio G, Barrett T, Jung DY, et al. The PPAR-FGF21 hormone axis contributes to metabolic regulation by the hepatic JNK signaling pathway. *Cell Metab* 2014;20:512-525.
- 38) Aguirre V, Werner ED, Giraud J, Lee YH, Shoelson SE, White MF. Phosphorylation of Ser307 in insulin receptor substrate-1 blocks interactions with the insulin receptor and inhibits insulin action. *J Biol Chem* 2002;277:1531-1537.
- 39) Kodama Y, Brenner DA. c-Jun N-terminal kinase signaling in the pathogenesis of nonalcoholic fatty liver disease: multiple roles in multiple steps. *HEPATOLOGY* 2009;49:6-8.
- 40) Cao W, Collins QF, Becker TC, Robidoux J, Lupo EG, Xiong Y, et al. p38 mitogen-activated protein kinase plays a stimulatory role in hepatic gluconeogenesis. *J Biol Chem* 2005;280: 42731-42737.
- 41) Kang HS, Okamoto K, Kim YS, Takeda Y, Bortner CD, Dang H, et al. Nuclear orphan receptor TAK1/TR4-deficient mice are protected against obesity-linked inflammation, hepatic steatosis, and insulin resistance. *Diabetes* 2011;60:177-188.
- 42) Li SZ, Zhang HH, Liang JB, Song Y, Jin BX, Xing NN, et al. Nemo-like kinase (NLK) negatively regulates NF-kappa B activity through disrupting the interaction of TAK1 with IKKbeta. *Biochim Biophys Acta* 2014;1843:1365-1372.
- 43) **An S, Zhao L, Shen L**, Wang S, Zhang K, Qi Y, et al. USP18 protects against hepatic steatosis and insulin resistance through its deubiquitinating activity. *HEPATOLOGY* 2017;66: 1866-1884.
- 44) **Yan F, Zhang X, Wang W**, Ji Y, Wang P, Yang Y, et al. The E3 ligase tripartite motif 8 targets TAK1 to promote insulin resistance and steatohepatitis. *HEPATOLOGY* 2017;65:1492-1511.

Author names in bold designate shared co-first authorship.

Supporting Information

Additional Supporting Information may be found at onlinelibrary.wiley.com/doi/10.1002/hep.30485/suppinfo.